# Axonal mitochondrial transport and potential are correlated

**Kyle E. Miller and Michael P. Sheetz***

Department of Biological Sciences, Room 713 Fairchild Building, Columbia University, New York, NY 10027, USA
*Author for correspondence (e-mail: ms2001@columbia.edu)

## Summary

Disruption of axonal transport leads to a disorganized distribution of mitochondria and other organelles and is thought to be responsible for some types of neuronal disease. The reason for bidirectional transport of mitochondria is unknown. We have developed and applied a set of statistical methods and found that axonal mitochondria are uniformly distributed. Analysis of fast axonal transport showed that the uniform distribution arose from the clustering of the stopping events of fast axonal transport in the middle of the gaps between stationary mitochondria. To test whether transport was correlated with ATP production, we added metabolic inhibitors locally by micropipette. Whereas applying CCCP (a mitochondrial uncoupler) blocked mitochondrial transport, as has been previously reported, treatment with antimycin (an inhibitor of electron transport at complex III) caused increases in retrograde mitochondrial transport. Application of 2-deoxyglucose did not decrease transport compared with the mannitol control. To determine whether mitochondrial transport was correlated with mitochondrial potential, we stained the neurons with the mitochondrial potential-sensing dye JC-1. We found that ~90% of mitochondria with high potential were transported towards the growth cone and ~80% of mitochondria with low potential were transported towards the cell body. These experiments show for the first time that a uniform mitochondrial distribution is generated by local regulation of the stopping events of fast mitochondrial transport, and that the direction of mitochondrial transport is correlated with mitochondrial potential. These results have implications for axonal clogging, autophagy, apoptosis and Alzheimer's disease.

Key words: Mitochondria, Statistical analysis, Antimycin, 2-Deoxyglucose, JC-1, Mitochondrial potential

## Introduction

Mitochondria undergo a continuous cycle of division and destruction, and have a half-life of approximately 1 month in the brain (Menzies and Gold, 1971). Mitochondria are synthesized in the cell bodies of neurons (Davis and Clayton, 1996) and are then transported down the axon (Hollenbeck, 1996). During aging, mitochondria become heterogeneous in potential and on average become more depolarized (Hagen et al., 1997). Depolarized mitochondria enter an acidic lysosomal compartment (Lemasters et al., 1998), where they are recycled by autophagy (Klionsky and Emr, 2000).

In neurons, mitochondria are distributed through a combination of transport and stopping events: over half of the mitochondria are stationary, whereas the rest move at velocities of 0.3–2.0 μm second$^{-1}$ (Allen et al., 1982; Hollenbeck, 1996; Ligon and Steward, 2000). Disruption of axonal transport leads to a nonuniform distribution of organelles along the axon. This occurs both when specific motor proteins are disrupted and in diseases such as Alzheimer's and Huntington's (Gunawardena and Goldstein, 2001; Gunawardena et al., 2003; Hurd and Saxton, 1996). Determining the baseline state of mitochondrial distribution is an important first step in understanding how disruptions in axonal transport occur.

Mitochondrial potential drives the production of ATP. The potential is generated by oxidative phosphorylation through the electron transport chain (Nicholls and Budd, 2000; Papa, 1996). Throughout the cell, mitochondrial potential is heterogeneous and varies in time and space in response to changes in metabolic demand (Bindokas et al., 1998; Collins et al., 2002; Overly et al., 1996; Smiley et al., 1991; Wong-Riley, 1989). A link is assumed, but the relationship between mitochondrial ATP production and transport remains unclear (Bereiter-Hahn and Voth, 1983; Friede and Ho, 1977; Hollenbeck et al., 1985; Martenson et al., 1995; Ochs and Hollingsworth, 1971; Ochs and Smith, 1971).

In this paper, we demonstrate the utility of novel techniques for the analysis of organelle distribution by showing that mitochondria are uniformly distributed along the axons. This distribution arises because rapidly transported mitochondria preferentially stop or dock in the middle of the gap between 'stationary' mitochondria. Drugs that inhibit mitochondrial function lead either to a blockade of transport or a doubling of retrograde mitochondrial transport. Analysis of mitochondrial potential during transport with the potential-sensitive dye JC-1 shows that ~90% mitochondria with high potential move towards the growth cone and ~80% of mitochondria with low potential move towards the cell body.

## Materials and Methods

### Cell culture

Coverslips were washed in concentrated nitric acid overnight, double-

distilled water (ddH$_2$O) for 30 minutes and stored in 100% ethanol. On the day of cell plating, coverslips were dried, incubated with 0.01% poly-L-ornithine (30-70 kDa; Sigma, St Louis, MO) for 30 minutes, and then washed three times for 15 minutes each in ddH$_2$O. Coverslips were then dried in a laminar flow hood under an ultraviolet lamp for 30 minutes, coated with 100 µl of 16 µg ml$^{-1}$ laminin in DMEM (Gibco, Carlsbad, CA) with glucose, L-glutamine and pyridoxine HCl, and without sodium pyruvate (Gibco) for 3 hours, and washed with DMEM (Banker and Goslin, 1998).

Neurons were derived from the dorsal root ganglia of embryonic-day-14 (E14) chicken embryos (Banker and Goslin, 1998). In brief, ganglia freed of surrounding membranes were incubated for 20 minutes at 37°C in 0.25% trypsin, 1 mM EDTA (Gibco). The trypsin was washed away, neurons dissociated by trituration, and plated onto poly-L-ornithine/laminin-coated glass coverslips at a density of ~2000 cells cm$^{-2}$ in DMEM as above with 10% fetal calf serum, 10 ng ml$^{-1}$ nerve growth factor (Sigma) and 1 mM sodium pyruvate.

Neuronal mitochondria were labeled with 0.1 µM Mitotracker Red CMXRos (Molecular Probes, Eugene, OR) in DMEM for 1 minute and then replaced with normal culture medium. Observations of the cells occurred at least 4 hours after the washout of Mitotracker.

## Image acquisition

Images were acquired on an IX 70 Olympus confocal microscope equipped with an Omnichrome laser and a PlanApo 60× oil (1.4 NA) objective.

## Flow chamber

Cells were observed in a flow chamber. The flow rate was set at 0.5 ml minute$^{-1}$ using DMEM with all supplements as described above. DMEM was equilibrated with 5% CO$_2$ and kept under a layer of mineral oil. Temperature was monitored using a probe embedded in the chamber and maintained at 37°C using a forced air heater.

## Drug application

Drugs were delivered focally using pipettes pulled on a Flaming/Brown Micropipette puller model P-97 (Sutter Instrument, Novato, CA). The pipettes were positioned and drug application was controlled using an Eppendorf micromanipulator 5171 and pressure regulator. Drug was applied in media containing Lucifer Yellow. The drug application was recorded in the green channel and then overlaid on the kymographs in Adobe Photoshop to show both the time of application and the area where the drug was applied. In these experiments, care was taken to ensure that the osmolarity of the solution was the same as that of the medium (320 mOsm). A 320 mOsm solution of 2-deoxyglucose (2-DG) in ddH$_2$O was made and then mixed with the medium to produce a solution of 200 mM 2-DG. Nonetheless, although the osmolarities of the solutions were the same, the relative concentrations of ions in the media (such as Ca$^{2+}$, Na$^+$ and K$^+$) were lower.

## Image processing

Time-lapse movies were acquired at a rate of one image every 2 seconds using the Fluoview software from Olympus. The laser power was set at the lowest possible setting and a polarizing filter in the laser path was adjusted to the point that allowed image acquisition but minimized photodamage and photobleaching. Fluoview files were opened in ImageJ, rotated so that the axons were horizontal and the images cropped. The stacks of images were then re-sliced and $z$-projected using the standard deviation option to make kymographs. Kymographs were opened in Adobe Photoshop, levels were adjusted and the image color depth was converted from 16 bits per pixel to 8 bits per pixel. The color was then inverted and lines tracing the path

of the mitochondria were drawn by hand in separate layers. Mitochondria trace files were saved and opened in NIH Image. The images were then thresholded and converted to 1 bit per pixel. The 'analyse particle' function of NIH image was then used to determine the length, angle and $x$-$y$ center of the mitochondrial paths. The results were then exported to Microsoft Excel and converted to a measure of transport in the units of mitochondria per second that was calculated by summing the total mitochondrial displacement in a single direction and then dividing this by the length of the axon and the observation duration. For the analysis of mitochondrial transport in response to application of drugs, the average number of mitochondria per second in each of the three regions (e.g. cell body side) in the pre-drug condition was individually set as 100% and used to normalize transport in the later conditions. The amount of transport for the early drug, late drug and post-drug conditions were averaged in terms of mitochondria per second and converted to a proportion of pre-drug levels of transport; the standard deviation for each of the regions and time points in combination with the number of experiments for each condition was used to calculate the individual 95% confidence intervals.

## Analysis of the goodness of fit of the Poisson distribution

The book *Biostatistical Analysis* (Zar, 1999) provides excellent explanations with examples of the statistics used in this paper. What follows is a complete but brief summary. To determine whether the distribution of mitochondria was uniform, random or clustered, the axon was divided into bins and the average number of mitochondria per bin, the standard deviation of the average and the variance were calculated. The type of distribution is determined by comparing average and variance: when a distribution is random, the variance is equal to the average; when uniform, the variance is less than the average; and, when clustered, the variance is greater than the average.

To determine significance levels, we used a $\chi^2$ analysis of the goodness of fit of the Poisson distribution. For this test, the frequency distribution of bins with a given number of mitochondria ($i=0,1,\ldots,k$) was determined ($f_i$) and compared with the frequency distribution predicted by the Poisson distribution ($\hat{f}_i$). The Poisson frequency distribution (Eqn 1) and the corresponding predicted frequency (Eqn 2), which is proportional to the total number of mitochondria ($n$), are calculated thus:

$$P(X) = \frac{e^{-\mu}\mu^X}{X!} \qquad (1)$$

where P($X$) is the probability of there being $X$ mitochondria in a bin, with µ being the average number of mitochondria per bin.

$$\hat{f}_i = [P(X_i)][n] \qquad (2)$$

The difference between the observed and predicted frequency distributions is used to generate the $\chi^2$ test statistic (Eqn 3),

$$\chi^2 = \sum_{i=1}^{k} \frac{(f_i - \hat{f}_i)^2}{\hat{f}_i} \qquad (3)$$

where $i$ is the number of mitochondria per bin, $k$ is maximum number of mitochondria per bin examined and the degrees of freedom is $v=k-2$.

## Vector sum analysis

To determine the average stopping position of mitochondria in relation to its two nearest neighbors', the normalized distribution of stopping events was converted to a circular distribution and the mean angle was calculated. The stopping events or angles ($n$) are denoted $a_1$ to $a_n$. The rectangular coordinates of the mean angle ($x$ and $y$) are given by Eqns

4, 5. The sample mean angle of the rectangular coordinates ($\bar{a}$) is given by Eqn 6. This approach allows an unbiased estimate of the average stopping position.

$$x = \sum_{i=1}^{n} \cos a_i \qquad (4)$$

$$y = \sum_{i=1}^{n} \sin a_i \qquad (5)$$

$$\tan \bar{a} = \frac{y}{x} \qquad (6)$$

Defining the magnitude of each vector angle as 1, the sum of the vectors ($R$) is given by Eqn 7.

$$R = \sqrt{x^2 + y^2} \qquad (7)$$

For a random collection of vectors, the predicted vector sum of a distribution is given by Eqn 8, with root-mean-square distance ($D_{rms}$) and $n$ equal to the number of vectors.

$$D_{rms} = \sqrt{n} \qquad (8)$$

This equation has been used to describe the displacement of a randomly diffusing particle in relation to its initial starting position (Feynman et al., 1963).

By comparing the magnitude of the predicted vector sum against the observed vector sum, the organization of events can be determined: when the distribution is uniform, $R < D_{rms}$; when the distribution is random, $R \approx D_{rms}$; and, when the distribution is clustered, $R > D_{rms}$. The significance level can then be calculated by determining the probability of that magnitude occurring by chance using a Monte Carlo simulation. To estimate the probability distribution of the sum of the vectors, 1000 individual sums of 58 vectors were calculated and then converted to a cumulative probability plot. The random numbers for the simulation used in Fig. 2 were obtained from http://www.random.org/.

Vector sum analysis can be thought of as finding the balance point in a disk. Wrapping the linear distribution of mitochondria around a circle gives the polar distribution (Fig. 2D). Imagine that each of the lines in the distribution is like a spoke on a bicycle tire. Random distributions of spokes will on average be imbalanced to a degree proportional to $D_{rms}$.

An independent means of testing for significance is to apply Rayleigh's test for circular uniformity (Zar, 1999), in which the $z$-statistic is given by Eqn 9.

$$z = \frac{R^2}{n} \qquad (9)$$

Although this test is useful for determining whether a circular distribution is clustered, it cannot distinguish between uniform and random distributions.

### Analysis of mitochondrial potential and transport

To determine mitochondrial potential during transport, neurons were stained with MitoTracker Green FM (Molecular Probes) at a final concentration of 500 nM in medium for 20 minutes and then incubated for 30 minutes in fresh medium. JC-1 (Molecular Probes) was then added at a final concentration of 3 μM for 5 minutes and then incubated in fresh media for 1 hour before viewing.

To quantify the difference in transport direction with mitochondrial potential, the number of transport events in a given direction was counted for both high- and low-potential mitochondria moving at a velocity greater than 0.6 μm second$^{-1}$ for at least 1 minute. In many cases, the mitochondria paused during transport. If the transport resumed and continued in the same direction, it was not counted as a second mitochondrion. If the mitochondrion reversed direction, it was counted as a new mitochondrion. Mitochondria that were red and slightly green owing to the Mitotracker FM green were considered to be of high potential. Mitochondria that were only green were considered to be of low potential.

## Results

### Mitochondrial distribution is uniform

To test whether mitochondrial distribution in the axon is random or ordered, we did a $\chi^2$ analysis of the goodness of fit of the Poisson distribution against the observed mitochondrial distribution (Zar, 1999). In our analysis, the distribution of the mitochondria over 10 minutes was analysed by picking a frame in a time-lapse movie (Fig. 1A), playing the movie back and forth, and examining the kymograph (Fig. 1B). When a cluster of Mitotracker stain moved together, it was defined as a mitochondrion. To distinguish individual mitochondria more easily, frames from the movies (e.g. Fig. 1A) were inverted in color and stretched by a factor of five on the $y$ axis (Fig. 1C). The centers of the mitochondria were then marked by hand as dots (Fig. 1D) and the positions of the dots were used for the analysis. The offset that is seen on the $y$ axis was ignored for this analysis because the spacing of mitochondria on different microtubules along the plane of one section of the axon would lead to a slight bias towards uniformity in distribution. To verify that mitochondria were not being under or over counted, we took the plot profile intensity distribution of the mitochondria along the axon (Fig. 1E), found the area under each peak (Fig. 1F) and compared the number of counted mitochondria with the area of the peaks (Fig. 1G). The high value for the coefficient of determination ($R^2=0.87$) between mitochondrial number and peak size indicated that we accurately estimated mitochondrial number along the axon (Fig. 1G).

Using the algorithm for marking mitochondrial position shown in Fig. 1D, we analysed the mitochondrial distribution in ten axons from seven different coverslips collected on six separate days. The average distance between the mitochondria was $6.2 \pm 6.08$ μm (average±s.d.). To determine whether the distribution was ordered, we used Chi-squared ($\chi^2$) analysis. With the average number of mitochondria per bin=1.0 ($n=354$ total mitochondria), we found a variance of $0.73 \pm 0.19$ (average±s.d., $n=10$ different neurons); number of categories ($k$)=5, degrees of freedom ($v$)=3; $\chi^2=20.5$; and a high confidence level [$P_{(20.5, 3)}=0.00013$] for a uniform distribution (Fig. 1H). Thus, with this high confidence level and the variance less than the average, we found that mitochondria are uniformly distributed along the axon.

The primary difficulty in the analysis was the definition of a mitochondrion. This arose because of both the resolution limit (~400 nm) of the light microscope and the heterogeneity of Mitotracker staining. Because of these limitations, it was not possible to determine objectively whether mitochondrial fusion or fission events occurred. The danger in this experiment was in underestimating the number of mitochondria along the axon, which could lead to the false conclusion that mitochondria have a uniform distribution. Therefore, we designed our analysis with a bias towards overestimating the number of
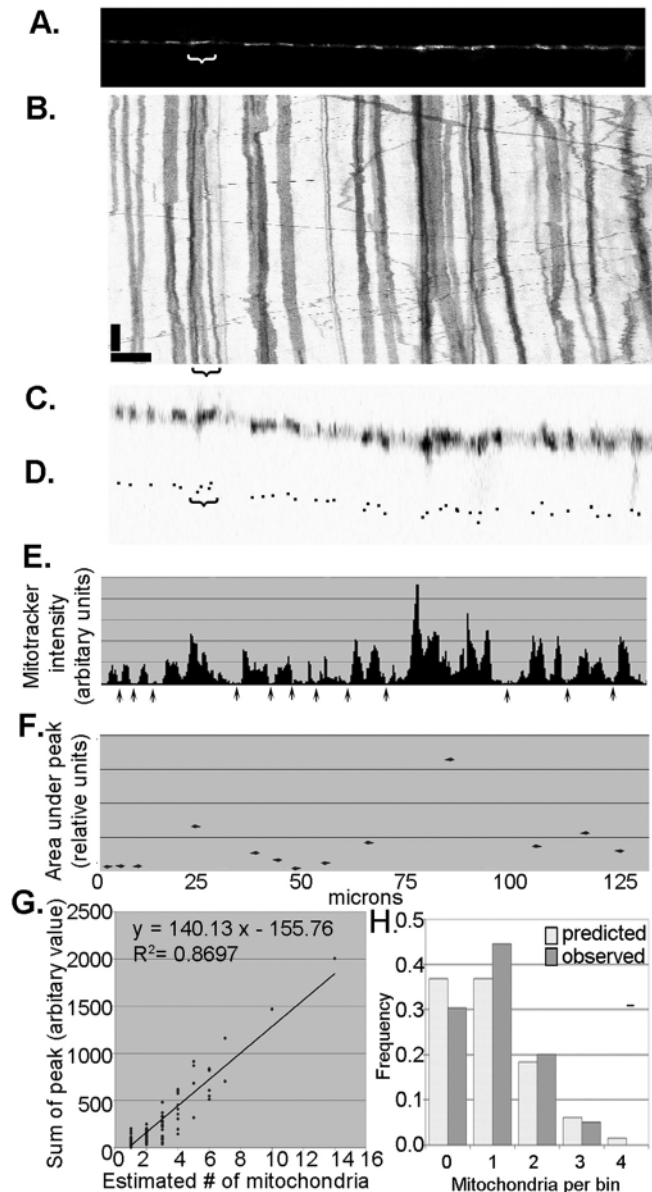
**Fig. 1.** Mitochondria are uniformly distributed along the axon.
(A) Distribution of Mitotracker-labeled mitochondria after 1 minute from a time-lapse movie. (B) Kymograph of the movie: horizontal bar=10 μm, vertical bar=1 minute. (C) Color-inverted image of (A) with height stretched by a factor of five in order to resolve the individual mitochondria better. (A-D) Brackets show a cluster of four mitochondria that can be resolved by analysis of the kymograph but cannot be resolved in the still picture. (D) Estimated centers of individual mitochondria, used for statistical analysis. (E) Intensity plot of the mitochondria, with arrows showing divisions between peaks. (F) Sum of the area for each of the peaks shown in (E). (G) Peak size vs estimated number of mitochondria. (H) Frequency distribution from the $\chi^2$ analysis of the goodness of fit of the predicted Poisson distribution vs the observed distribution.

mitochondria. In an initial analysis that did not resolve closely spaced mitochondria, both the calculated degree of uniformity and the significance levels were higher. A potential concern was the use of the confocal microscope. Nonetheless, images were taken with the confocal aperture at its widest position and focusing the objective up and down on the axon did not lead to the appearance or disappearance of mitochondria in a single region. Finally, although there is a significant degree of uniformity in distribution, it is also obvious that there is a random component.

## Quantification of fast mitochondrial transport

To define the normal level of mitochondrial transport, kymographs were generated and line traces were made of the moving mitochondria. By analysing the traces, we could determine the flux of the mitochondria, the velocity of transport and the number of mitochondria in motion. In our axons, the flux during pre-drug conditions (3765 total lines analysed for 15 axons and 150 minutes of recordings) was 0.030±0.014 mitochondria second$^{-1}$ (average±s.d.) in the plus direction and 0.036±0.023 mitochondria second$^{-1}$ (average±s.d.) in the minus direction. These numbers represent the number of mitochondria that pass a given point along the axon over time. In this data set, the velocity of transport in the plus direction was 0.93±0.55 μm second$^{-1}$ (average±s.d.), and the velocity of transport in the minus direction was –0.99±0.7 μm second$^{-1}$ (average±s.d.). Based on a paired two-tailed Student's $t$-test ($P$=0.403), the results for the plus and minus end directed transport were not significantly different.

To compare the size of the moving and stationary mitochondria, the sum of the Mitotracker staining pixel intensity for all stationary and moving mitochondria in an axon was calculated and then normalized to 1 for the stationary mitochondria for each of seven neurons. The adjusted arbitrary average pixel intensity for the stationary mitochondria was 1±0.56 (average±s.d., $n$=215 mitochondria) with a range of 0.08 to 2.87, and that for the moving mitochondria was 0.44±0.42 (average±s.d., $n$=120 mitochondria) with a range of 0.08 to 2.33. The moving mitochondria were significantly smaller based on Student's two-tailed, unequal variance $t$-test ($P$=9.4×10$^{-22}$). Although the overall ranges of mitochondrial size in the stationary and moving population were similar, larger mitochondria tended to move less frequently than smaller mitochondria. Mitochondrial transport has previously been expressed as percentages of mitochondria moving. Previous studies have reported that 25–75% of mitochondria are in motion (Ligon and Steward, 2000; Morris and Hollenbeck, 1993), and we find that 25.8±16.8% (average±s.d.) of the mitochondria were in motion (i.e. velocity > 0.6 μm second$^{-1}$, $n$=507 mitochondria from ten axons).

## Moving mitochondria stop in the gaps between stationary mitochondria

During the observational interval of several hours, alterations in mitochondrial distribution occurred primarily through movements mediated by fast axonal transport. We reasoned that, by observing where mitochondria stopped in relation to surrounding stationary mitochondria, we could determine whether the stopping events created a more-or-less uniform distribution. To determine whether stops during fast axonal transport occurred randomly or clustered in the gap between stationary mitochondria, we analysed the position of the stopping points in relation to stationary mitochondria. Nine
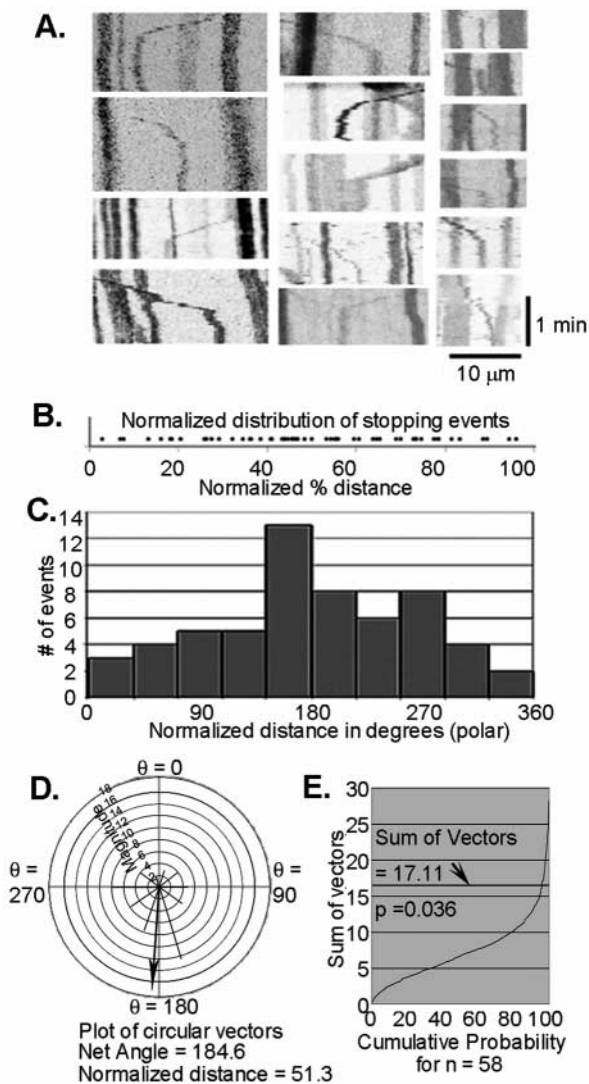
**Fig. 2.** Mitochondrion transported by anterograde and retrograde transport dock in the middle of the gap between stationary mitochondria. (A) Examples of mitochondria pausing during fast axonal transport. (B) Normalized distribution of mitochondrial stops relative to the two closest stationary mitochondria ($n$=58 stopping events). (C) Histogram analysis of the relative position of the stops in relation to the two closest mitochondria ($n$=58 stopping events). (D) Circular histogram of stopping events. Line with arrowhead shows the sum ($R$) and net angle of the vectors. (E) Cumulative probabilities of the vector sums of 58 random events generated by Monte Carlo simulation. From this, we estimate the probability of the observed clustering shown in (C) to be $P$<0.036.

axons were observed for a total of 4 hours and 58 stops were recorded. Fig. 2A shows 15 examples of the stops.

We calculated the positions of the stops relative to the surrounding mitochondria in terms of the proportion of the distance between the nearest stationary mitochondria [i.e. a mitochondrion that stopped very close to the leftmost (toward the cell body) stationary mitochondrion might have had a distance value of 5%]. The normalized distribution of the stopping events (Fig. 2B,C) showed they cluster between stationary mitochondria. To determine whether the observed

clustering of pauses between stationary mitochondria was statistically significant, a $\chi^2$ analysis of the goodness of fit of the Poisson distribution was performed. For this analysis, the number of events [$n$=58, average number of mitochondria per bin=1.0, variance=1.33; degrees of freedom ($v$)=4; $\chi^2$=12.26; confidence level ($P_{12.26, 4}$)=0.015]. Thus, with this high confidence level and a variance greater than the average, $\chi^2$ analysis demonstrates that there was significant clustering of the stops.

### Vector sum analysis: determining the average stopping position

The $\chi^2$ analysis of mitochondrial stopping events was limited to measuring the amount of clustering, not its location. Although visual inspection of the distribution of stops showed that mitochondria clustered in the middle of the gap (Fig. 2B,C), we applied a second statistical test, vector sum analysis, to determine the center of the cluster of stopping events. For the 58 observations, the angle of the sum of the vectors was 184.6°. Converting the angle back to the normalized position distribution gave an average stopping position value of 51.3% of the distance between the two closest stationary mitochondria (Fig. 2D).

The predicted magnitude of the sum of the vectors for our data from Eqn 7 was 7.6. The observed magnitude of the sum of the vectors was $R$=17.1. Because $R>D_{rms}$, the distribution is clustered. To determine the significance level, a Monte Carlo simulation was used to generate 1000 examples of the sum of 58 random vectors (Fig. 2E). Out of the 1000 randomly generated vector sums of $n$=58, the average of sums was 7.3±4.42 (average±s.d.), and 36 had a sum greater than 17.1. Based on the Monte Carlo analysis, we estimate that the probability of obtaining the observed distribution by coincidence was approximately 0.036. Using Rayleigh's test for circular uniformity (Eqn 9), $z$=5.04, and using the conservative value of $n$=55 gives a significance of between 0.01 and 0.005. The strength of vector sum analysis is that it gives both the true average stopping position and an estimate of the randomness of the distribution.

Comparison of the results from vector sum analysis with the $\chi^2$ analysis of the goodness of fit of the Poisson distribution showed good agreement in the levels of significance. From these tests, we conclude that stopping or docking events occurred at non-random sites and contributed in generating the observed uniform distribution of mitochondria along the axon.

### Antimycin activates retrograde mitochondrial translocation

Antimycin blocks electron transport at complex III, which leads to a depolarization of the mitochondrial potential and a decrease in mitochondrial ATP production (Bindokas et al., 1998; Collins et al., 2002; Nicholls and Budd, 2000; Pilatus et al., 2001; Reers et al., 1991). To test the effect of an inhibitor of the electron transport chain on fast mitochondrial transport, we added drug to the medium that was flowing past an axon with a micropipette. When we included fluorophores in the pipette effluent, we found that they typically bathed a 15-30 μm stretch of the axon. Application of 100 μM antimycin (Fig. 3A, blue) led to an immediate, significant, transient increase in the number of retrogradely transported mitochondria (Fig. 3B,D). In these
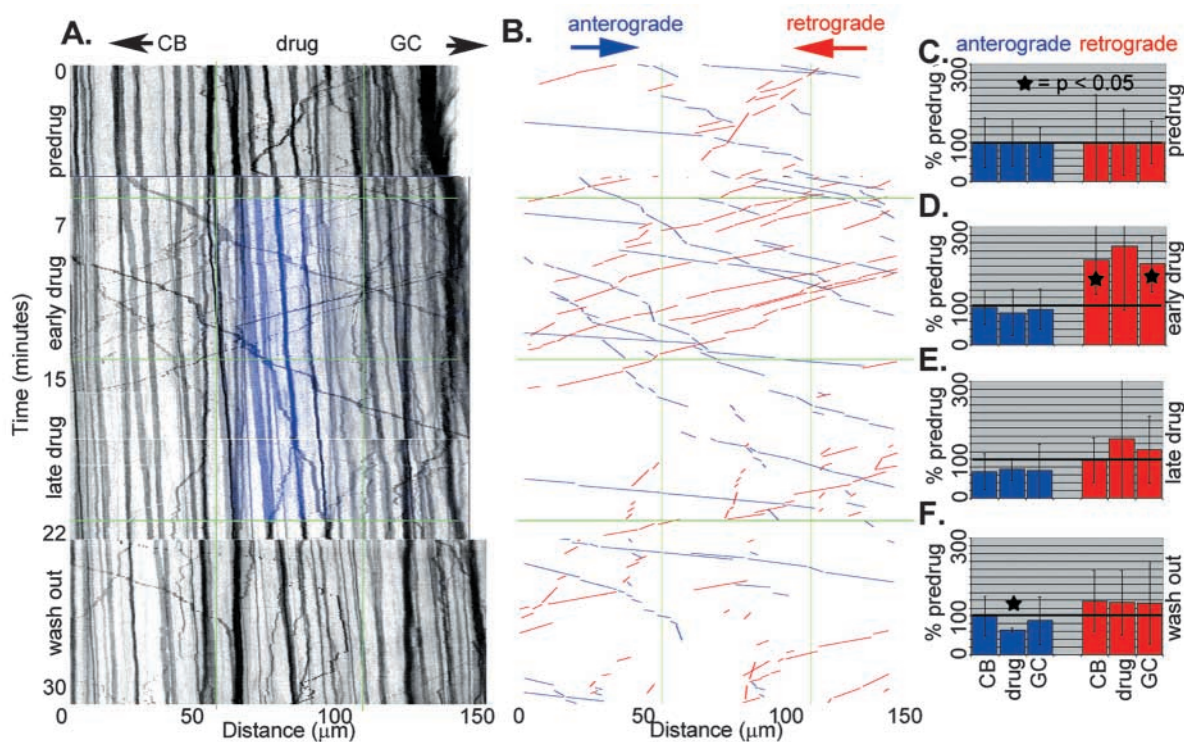
**Fig. 3.** Antimycin, an inhibitor of the electron transport chain, doubles retrograde transport. (A) Kymograph of distribution and movements of Mitotracker-labeled mitochondria. Transport of the mitochondria was observed for 5-10 minutes for the pre-drug, early drug, late drug and washout application conditions as delineated by the horizontal green lines. The position and time of drug application (100 μM antimycin and Lucifer Yellow in DMEM) is shown in blue. The length of the axon was also divided into three sections with reference to the position of drug application (cell-body side, CB; position of drug application, drug; growth-cone side, GC). (B) Hand-drawn traces of anterograde (blue) and retrograde (red) movements used to quantify the mitochondrial transport. (C-F) Normalized anterograde and retrograde transport. Error bars are the normalized 95% confidence intervals (*n*=5 experiments). (D) There is significant transient increase in retrograde transport but no effect on anterograde transport. (E) After 5 minutes, retrograde transport returns to baseline levels.

experiments, five axons were analysed for 164 minutes, and 2935 traces were measured. After approximately 5 minutes, translocation decreased to pre-drug levels (Fig. 3E). Upon removal of drug, retrograde transport was not significantly different than before the drug was added, although anterograde transport decreased slightly (Fig. 3F). These experiments suggest that disruption of mitochondrial ATP production or potential can lead to an increase in retrograde mitochondrial transport.

### 2-DG modestly decreases both anterograde and retrograde mitochondrial translocation

2-DG is a competitive inhibitor of glucose metabolism that can decrease glycolytic ATP production. Application of 2-DG (200 mM) in DMEM with Lucifer Yellow (Fig. 4A, blue) leads to a ~50% reduction in both anterograde and retrograde transport past the point of drug application (Fig. 4A,B,E). A total of five axons were analysed for 139 minutes and 1463 traces were measured. Although the concentration of 2-DG required to produce an effect was high, the osmolarity of the 2-DG solution was carefully matched to the bath medium. Nonetheless, because the osmolarity was held constant, the applied concentrations of Na$^+$, K$^+$ and the other ions were decreased. Although the results of this experiment might appear to be consistent with the hypothesis that inhibition of glycolysis halts fast axonal transport (Ochs and Smith,

1971), we attribute this effect to local alteration of the ionic balance.

### Mannitol also decreased both anterograde and retrograde mitochondrial translocation

As a control for 2-DG, we added mannitol (200 mM) in DMEM plus Lucifer yellow with osmolarity maintained at 320 mM (Fig. 5A, blue). Mannitol, like 2-DG, would alter the local medium composition, but mannitol is not known to affect cell metabolism directly (Fishman et al., 1977). Nonetheless, iso-osmotic replacement of NaCl with mannitol has been reported to increase intracellular Ca$^{2+}$ levels (Borgdorff et al., 2000). Application of mannitol led to a decrease in both anterograde and retrograde transport (Fig. 5A,B,E). Washout of drug (Fig. 5F) resulted in rapid resumption of transport but not quite back to pre-drug levels. The rapid reversibility of the effect indicates that the decrease in transport was not due to damage of the axon. Because 2-DG and mannitol had similar effects on mitochondrial transport but not on metabolism, we concluded that the decrease in transport seen with 2-DG was not due to alteration of metabolism.

### Uncoupling agent CCCP does not increase retrograde mitochondrial transport

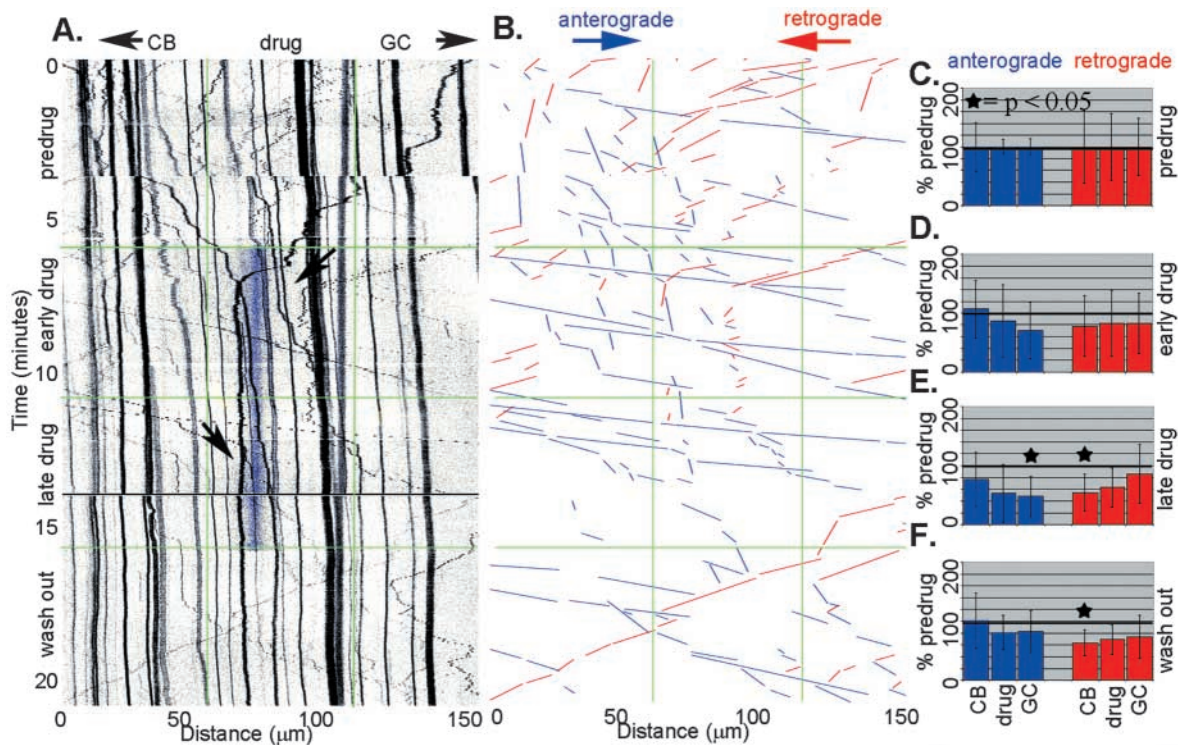Uncouplers of the mitochondrial proton gradient, like carbonyl

**Fig. 4.** Application of 2-DG, a competitive inhibitor of glycolysis, has a minor effect on mitochondrial transport. (A) Kymograph of distribution and movements of Mitotracker-labeled mitochondria. The position and time of drug application (200 mM 2-DG, and Lucifer Yellow in DMEM) is shown in blue. (B) Hand-drawn traces of anterograde (blue) and retrograde (red) movements used to quantify the mitochondrial transport. (C-F) Normalized anterograde and retrograde transport. Error bars are the normalized 95% confidence intervals (*n*=5 experiments). (D) Decreases in anterograde and retrograde transport start but do not reach significant levels. (E) After 5 minutes of drug application both anterograde and retrograde transport are modestly (*P*<0.05) decreased for each direction of transport past the point of drug application. (F) Anterograde and retrograde transport after drug application is stopped.

cyanide m-chlorophenylhydrazone (CCCP), accelerate oxygen uptake and $H^+$ pumping, and depolarize mitochondria, which inhibits production of ATP (Nicholls and Budd, 2000; Pilatus et al., 2001). CCCP has been previously reported to inhibit organelle motility but its effect has been attributed to an action besides the depolarization of mitochondria (Hollenbeck et al., 1985). Nonetheless, it was used to determine whether mitochondrial transport could be effectively stopped in the axon and to compare its effect against antimycin. CCCP (1 mM) mixed with Lucifer Yellow to visualize the region of drug application (Fig. 6A, blue) was locally applied to five axons. For these experiments, the total time of observation was 193 minutes, and 1877 measurements of mitochondrial movements were recorded. Immediately after drug addition (Fig. 6A,B,D), both anterograde and retrograde translocation decreased. 10 minutes after addition (Fig. 6E), transport was decreased by ~ 80%. Washout of drug (Fig. 6F) resulted in rapid resumption of transport but not quite back to pre-drug levels (Fig. 6F). The rapid reversibility of the effect suggests that the decrease in transport was not due to damage of the axon. Notably, the addition of CCCP did not lead to an increase in retrograde mitochondrial transport.

### Direction of fast mitochondrial transport is correlated with mitochondrial potential

To determine the relationship between mitochondrial potential

and transport, axonal mitochondria were stained with the mitochondrial-potential-sensitive dye JC-1 (Reers et al., 1991). In contrast to Mitotracker Red CMXRos under the conditions we used, observation of JC-1-stained neurons showed a rapid degradation in their health and rapid loss of red J-aggregate staining. Retraction of the axons was a common occurrence during observation, and the low light levels that were used to acquire the images made it difficult to resolve the depolarized mitochondria. To minimize these problems, observations were limited to 10 minutes and Mitotracker FM-green was used to aid in the visualization of the mitochondria with low potential.

Along the length of the axon, the stationary mitochondria had a mixed potential (Fig. 7D). Although care was taken to minimize the amount of illumination, a consistent shift in the ratio of red/green occurred during the course of observation (Fig. 7D,F,J,L). We were not able to determine whether this was due to photobleaching or reflected a depolarization of the mitochondria caused by photodamage (Huser and Blatter, 1999). Although it might appear in the kymographs that the mitochondria that are transported towards the growth cone have a higher potential than the stationary mitochondria, examination of Fig. 7D,J against the first minute of observation shows that, at the beginning of the observations, some of the stationary mitochondria have as high a potential as mitochondria moving towards the growth cone.
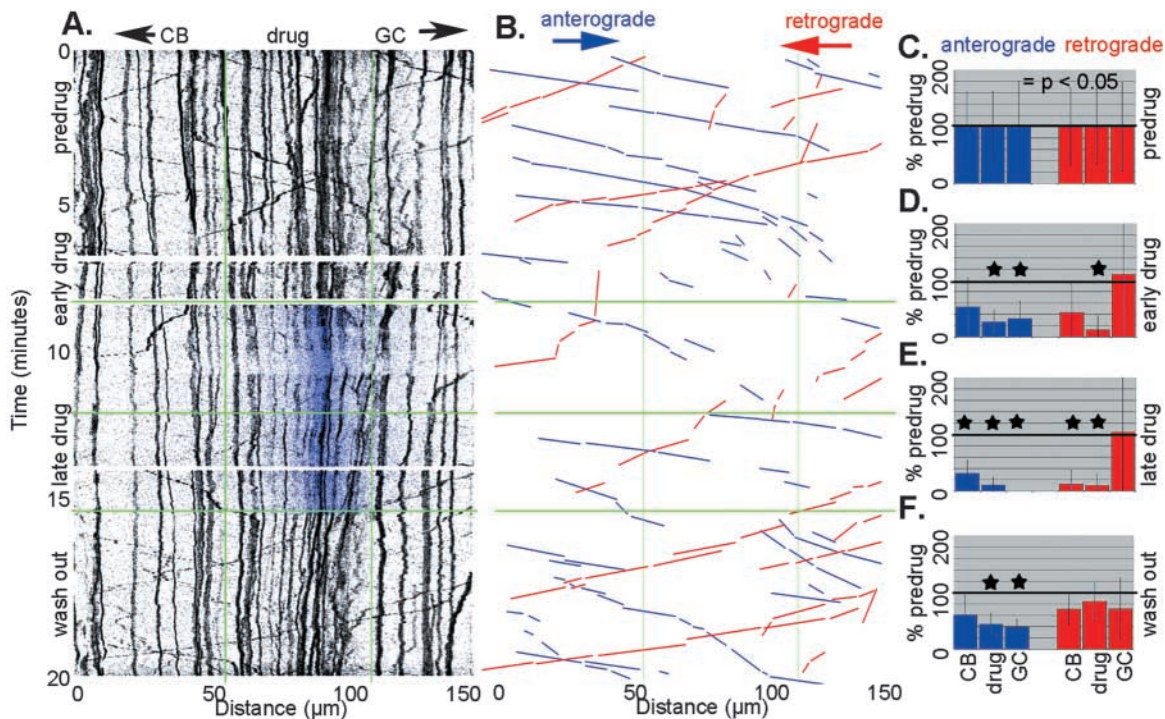
**Fig. 5.** Local application of mannitol, an ionic control for 2-DG, suggests that inhibition of transport by 2-DG is not due to inhibition of glycolysis. (A) Kymograph of distribution and movements of Mitotracker-labeled mitochondria. The position and time of drug application (200 mM mannitol and Lucifer Yellow in DMEM) is shown in blue. (B) Hand-drawn traces of anterograde (blue) and retrograde (red) mediated movements used to quantify the mitochondrial transport. (C-F) Normalized anterograde and retrograde transport. Error bars are the normalized 95% confidence intervals (*n*=5 experiments). (D-E) After 5 minutes of drug application, both anterograde and retrograde transport are significantly (*P*<0.05) decreased for each direction of transport past the point of drug application. (F) Anterograde and retrograde transport increase after drug application is stopped.

The mitochondrial transport in 12 neurons was examined for a combined total of 103 minutes (Fig. 7) and a consistent asymmetry was observed in the transport of high- versus low-potential mitochondria. Examples are shown of mitochondrial transport in the middle of the axon (Fig. 7A-F), and close to the growth cone (Fig. 7G-L). Over the period of observation, we recorded a total of 94 quickly transported mitochondria with high potential (Fig. 7A,G, red lines). Of these, 84 (89%) moved towards the growth cone. Using a two-tailed binomial test (Zar, 1999), we found that there was a significant bias in directionality of transport ($P<1\times10^{-15}$). For the mitochondria with low potential, we recorded a total of 61 quickly transported mitochondria (Fig. 7A,G, green lines). Of these, 50 (81%) moved towards the cell body ($P<4.5\times10^{-7}$). Exceptions are pointed out with a triangle for a mitochondrion with a low potential moving towards the growth cone (Fig. 7A-C,E), and an arrow to a high-potential mitochondrion moving towards the cell body (Fig. 7A-C,E). The transport and accumulation of high-potential mitochondria into the growth cone is shown by a double circle (Fig. 7H). Alterations in mitochondrial potential also occurred during observation. A particularly dramatic mitochondrial depolarization event from a very high potential to a moderate potential is circled in Fig. 7B,C,E. Although there were exceptions, we found that mitochondria with a high potential moved towards and accumulated in the growth cone, and mitochondria with a low potential were transported towards the cell body.

## Discussion

### Overview

Long-term tracking of mitochondria has enabled us to establish that their distribution is uniform along the axon (Fig. 1). To determine whether there is a physiologically relevant local regulation of fast axonal transport, the stopping events of fast transported mitochondria were analysed (Fig. 2). Immobilization events were clustered in the middle of gaps between stationary mitochondria. To test the effect of local inhibition of ATP production on transport, drugs were locally applied along the axon with a micropipette. Treatment with antimycin caused a local doubling of retrograde mitochondrial transport (Fig. 3). Application of 2-DG did not decrease transport compared with the mannitol control (Figs 4, 5). CCCP locally halted both anterograde and retrograde fast mitochondrial transport (Hollenbeck et al., 1985), but did not lead to an increase in retrograde transport (Fig. 6). Analysis of mitochondrial potential and transport with the dye JC-1 shows that mitochondria with a high potential move towards the growth cone and mitochondria with a low potential move towards the cell body (Fig. 7). Together, these experiments provide a means of analysing organelle distribution to establish that the distribution of mitochondria along the axon is uniform through the regulation of fast axonal transport. Furthermore, we found that mitochondria with high potential are transported out into the axon to replace old or damaged mitochondria with low potential.
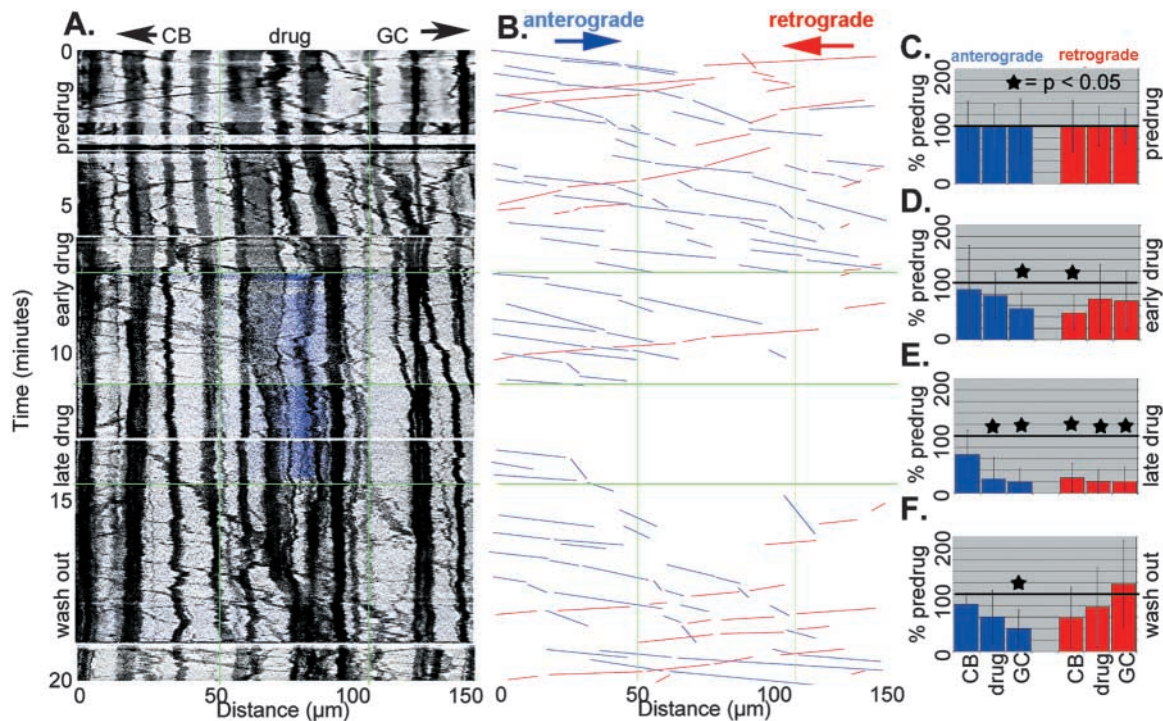
**Fig. 6.** The mitochondrial uncoupler CCCP decreases both kinesin- and dynein-mediated transport but does not lead to a transient rise in retrograde transport. (A) Kymograph of distribution and movements of Mitotracker-labeled mitochondria. The position and time of drug application (1 mM CCCP and Lucifer Yellow in DMEM) is shown in blue. (B) Hand-drawn traces of anterograde (blue) and retrograde (red) mediated movements used to quantify the mitochondrial movements. (C-F) Normalized anterograde and retrograde mediated transport. Error bars are the normalized 95% confidence intervals ($n$=5 experiments). (D,E) There is significant decrease in both anterograde and retrograde mediated transport. (F) After washout, transport recovers.

## Kymographic analysis and image acquisition

Kymographs (Zhou et al., 2001) are a concise means of data presentation that provide several advantages for motion analysis. In particular, they aid in the visualization of rare and subtle events such as mitochondrial docking and small shifts in position. Although particle-tracking programs are superior for detailed analysis of individual mitochondria, difficulties with this technique arise when there are variations in intensity or morphology, or when mitochondria pass each other. By contrast, because noise is averaged in the *y* dimension and non-coherent in the time dimension, kymographs allow mitochondrial tracking from a series of images with low signal-to-noise ratios, variations in mitochondrial intensity and past stationary mitochondria.

Photodamage limits the acquisition of images of mitochondria with high temporal and spatial resolution (Ligon and Steward, 2000). By using a closed flow chamber to wash out free radicals and to maintain DMEM with 5% $CO_2$, minimizing illumination, and kymographic analysis, continuous observation of mitochondria could be made for at least 1 hour with an image acquisition rate of 0.5 Hz. Mitotracker FM-green, Mitotracker Orange, JC-1 and DiOC6 were not routinely used for long-term observation because of problems with viability and photobleaching (Rottenberg and Wu, 1998). Although Mitotracker Red CMXRos was not usable for long-term imaging following the manufacturer's guidelines (Minamikawa et al., 1999), axons could be routinely imaged for 30 minutes by reducing the time of incubation with

the dye, allowing the cells to rest for a several hours after drug application and using minimal illumination.

## Statistical analysis

This is the first quantitative examination of mitochondrial distribution (Fig. 1) and provides a way to understand axonal clogging and other disruptions in organelle distribution (Gunawardena and Goldstein, 2001; Gunawardena et al., 2003; Hurd and Saxton, 1996). The power of this analysis is that it provides the first direct evidence that mitochondrial distribution is regulated along the length of the axon. Although $\chi^2$ analysis of the stopping events showed that they were clustered in the middle of the gap between previously docked mitochondria, this test gave no information about the average stopping position. In particular, stopping events clustered in the middle of the gap or a bimodal distribution of stopping events would show the same average stopping position in the middle of the gap while reflecting very different distributions. To overcome this problem, we converted the linear distribution of stopping events to a circular distribution and confirmed that, on average, the mitochondria stop in the middle of the gap (Fig. 2). Both Rayleigh's test (Zar, 1999) and vector sum analysis independently confirmed that there was significant clustering of the stopping positions of the mitochondria. Although Rayleigh's test is well established, it gives no information about whether a circular distribution is uniform or random (Zar, 1999). By contrast, vector sum analysis provides general means of testing

**Fig. 7.** The direction of mitochondrial transport is correlated with mitochondrial potential as assayed with JC-1 and Mitotracker FM-green. (A) Hand-drawn traces of anterograde and retrograde mitochondrial movements from the middle of an axon. Red and green lines represent the movements of mitochondria with a correspondingly high or low ratio of red/green staining. The arrow and triangle point to two mitochondrial traces that are exceptions to the correlation between potential and direction of transport. The vertical bar equals 1 minute and the horizontal bar equals 10 μm. (B) Color-inverted kymograph of red channel showing movements of mitochondria with high potential as assayed by JC-1. The circle indicates a mitochondrion undergoing a decrease in potential. (C) Color-inverted kymograph of green channel showing movements of JC-1/Mitotracker-FM-green-stained mitochondria. (D) The first frame of the time-lapse sequence shows the mixed polarity of mitochondria along the axon. (E) Overlay of red and green channels. (F) The last frame of the time-lapse sequence. (G) Hand-drawn traces of mitochondrial movements close to the growth cone. (H) Color-inverted kymograph of red channel. The double circle illustrates accumulation of mitochondria with high potential at the growth cone. (I) Color-inverted kymograph of green channel. (J) The first frame of the time-lapse sequence. (K) Overlay of red and green channels. (L) The last frame of the time-lapse sequence.
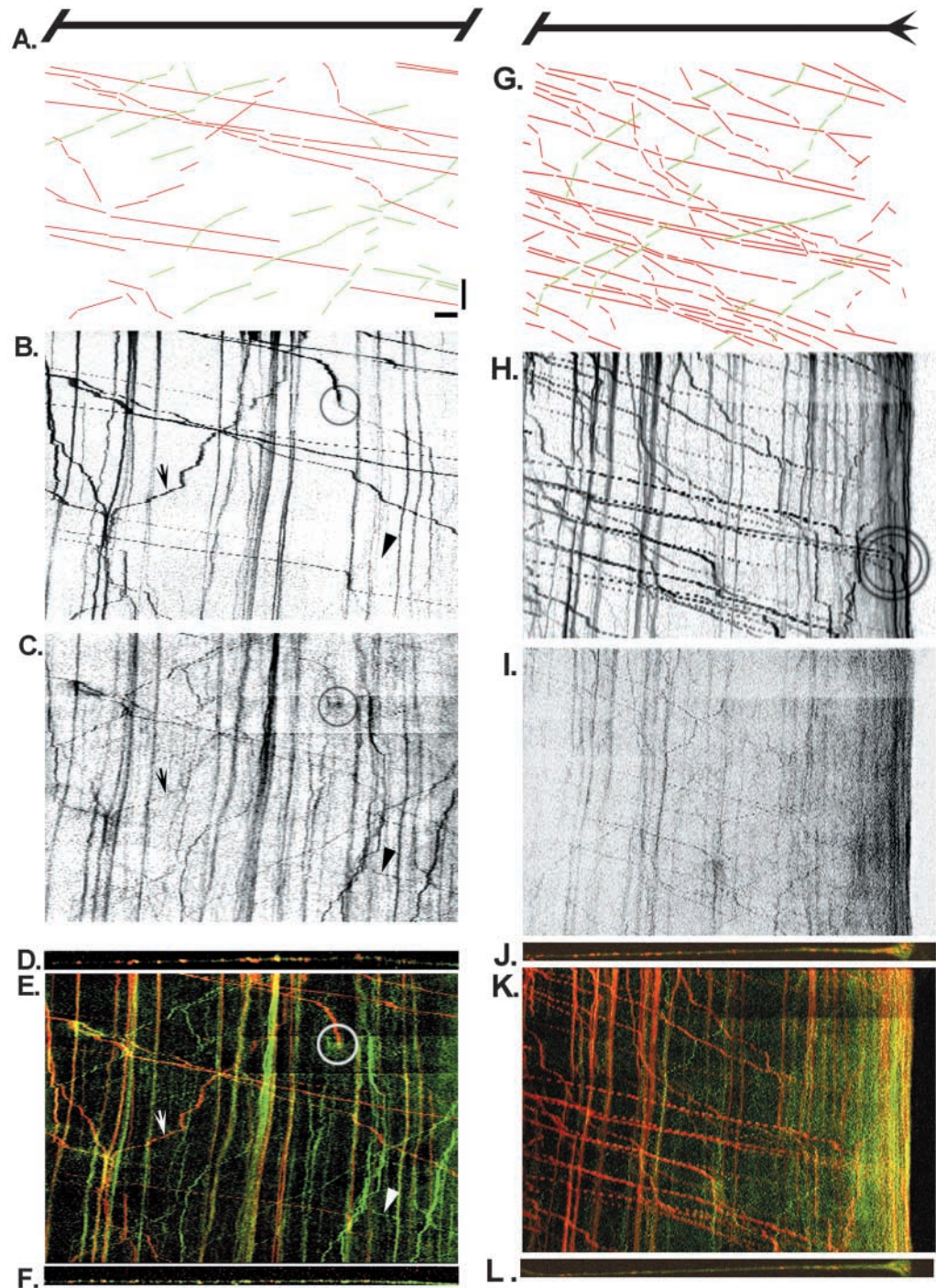
randomness in distributions that can be converted to a circular format. Together these tools provide a way to measure organelle distribution and to quantify effects seen in neuronal diseases.

## Mitochondrial scanning of the axon

Although the analysis of mitochondrial stopping positions demonstrates a significant tendency for mitochondria to stop in the gaps, individual mitochondria can pass multiple gaps in between mitochondria without stopping. Thus, we suggest that individual mitochondria have different levels of sensitivity to

the signal to stop, or that the sensitivity can change over time. This stochastic aspect of transport might play an essential role by allowing mitochondria to scan large lengths of the axon and yet maintain the ability respond to regions of high local demand.

## Antimycin and activation of retrograde transport

Antimycin inhibits complex III in the electron transport chain (Kaniuga et al., 1968), which leads to mitochondrial depolarization (Bindokas et al., 1998) and eventually apoptosis (Tzung et al., 2001). The observed increase in

retrograde mitochondrial transport supports a model in which trauma or age-dependent damaging of mitochondria activates a signal for retrograde transport (Xue et al., 2001). Further support for this model comes from observations of perinuclear clustering mitochondria following the induction of apoptosis (De Vos et al., 1998), and from our observation that mitochondria with a low potential are selectively transported towards the cell body (Fig. 7). Nonetheless, with respect to these experiments there are several cautions to note.

Activation of retrograde transport by antimycin was transient and most mitochondria in the region of drug application remain stationary (Fig. 3). The transient increase in mitochondrial transport following inhibition of complex III might reflect a concentration-dependent activation of transport or a clearing of sensitive mitochondria. Although the increased retrograde transport might be due to depolarization of the mitochondria, it is possible that transport by antimycin is activated through a pathway involving the induction of apoptosis, such as by interference with Bcl-X/Bcl-2 (Desagher and Martinou, 2000; Tzung et al., 2001). However, the time dependence and reversibility of the effects of antimycin indicate that they are not correlated with an irreversible step towards apoptosis. Finally, as discussed below, application of 2-DG or CCCP did not lead to an increase in retrograde transport (Figs 4, 6). The observation that antimycin activates retrograde transport (Fig. 3) is consistent with the hypothesis that mitochondrial potential (Fig. 7) is important for the regulation of the direction of transport but, nonetheless, the link appears to be indirect.

### Ionic blockade of fast axonal transport?

Mitochondrial transport was inhibited both by mannitol and 2-DG (Figs 4, 5). The results of the mannitol experiment correlate with a disruption of the ionic balance, either $Na^+$-$K^+$ or $Ca^{2+}$. The relatively weak effect of 2-DG differs from the previously reported blockade of fast mitochondrial transport with the glycolytic inhibitor iodoacetic acid (Ochs and Smith, 1971), but the results of that experiment might be due to iodoacetic acid's direct inhibition of the microtubule motors (Martenson et al., 1995).

Prior work looking at the effect of iso-osmotic replacement of NaCl with mannitol shows that replacement does not cause changes in overall metabolic activity (Fishman et al., 1977) but does consistently increase intracellular $Ca^{2+}$ levels and electrical excitability (Borgdorff et al., 2000). Although calcium is a requirement for axonal transport, increases in cytoplasmic calcium levels also inhibit mitochondrial transport (Kanai et al., 2001; Kanje et al., 1981; Kendal et al., 1983). Because mitochondria are involved in calcium regulation (Budd and Nicholls, 1996; Rizzuto, 2001), it will be important to understand how intracellular ionic composition modulates mitochondrial transport.

### Uncouplers and the blockade of axonal transport

The inhibition of transport by CCCP (Fig. 6) is reported to be a non-specific effect independent of mitochondrial depolarization (Hollenbeck et al., 1985). Other uncouplers, such as 2,4-dinitrophenol (DNP), carbonyl cyanide p-trifluoromethoxyphenyl-hydrazone (FCCP) and pentachloro-phenol (PCP), increase or have no effect on mitochondrial transport (Bereiter-Hahn and Voth, 1983; Hollenbeck et al., 1985). Because CCCP is one of the most effective uncouplers (Cunarro and Weiner, 1975) and can cause mitochondria to become consumers of ATP (Nicholls and Budd, 2000), its effect might occur because it lowers local ATP levels such that transport cannot be sustained. Additionally, the increases in calcium that have been observed with CCCP application might inhibit transport (Nicholls and Budd, 2000). The different effects of CCCP and other blockers of mitochondrial ATP production could be used to advantage to help determine the role of axonal transport during apoptosis.

### Local drug application

Although our method of locally applying drugs to a discrete region of the axon in cultured DRG neurons is an excellent means of addressing questions about local effects of disrupting mitochondrial transport, it is not suitable for a systematic analysis for at least three reasons. First, the drug concentration that reaches the axon is not tightly controlled, because the drugs are applied from a pipette in a flow chamber. Second, these experiments are technically challenging and attaining large numbers of replicates at a single concentration is not possible in a reasonable time scale. Third, an internal control using a different organelle should be used to determine whether effects on mitochondrial transport are specific. We attempted such a control using Lysotracker and DiOC6 for endoplasmic reticulum (Terasaki and Reese, 1992) but found few lysosomes in the axon and problems of toxicity with DiOC6. The use of green- and red-fluorescent-protein-labeled organelles in an easily transfectable cell line or in a genetic system (Stowers et al., 2002) in combination with bath application of the drugs or genetic knockouts would be the ideal approach for detailed analysis.

### Spatial relationship between mitochondrial demand and potential

Mitochondrial potential is spatially correlated with metabolic demand. Growth cones (Overly et al., 1996), synapses (Wong-Riley, 1989) and the cell periphery of hepatocytes (Collins et al., 2002) are all enriched with high-potential mitochondria. Although increases in mitochondrial potential in response to synaptic activity have been demonstrated (Bindokas et al., 1998), the contribution of transport has not been shown previously. Our observation that mitochondria with high potential are transported towards the plus ends of microtubules (Burton and Paige, 1981; Ferhat et al., 1998; Ha, 1970; Heidemann et al., 1981) and accumulate in the growth cone (Fig. 7H) can account in part for the correlation between mitochondrial potential and distribution.

### Autophagy, apoptosis, and retrograde transport

Mitochondria that depolarize either spontaneously or because of apoptosis show perinuclear clustering (De Vos et al., 1998; Desagher and Martinou, 2000) and are targeted for elimination by autophagy (Lemasters et al., 1998; Xue et al., 2001). Depolarized mitochondria are thought to display or release a factor that leads to their specific removal (Xue et al., 2001).

The transport of depolarized mitochondria towards the cell body (Fig. 7) might be an early step in the autophagy process (Hollenbeck, 1993; Hollenbeck and Bray, 1987; Klionsky and Emr, 2000) and could play an important role in clearing damaged mitochondria from the axon and in apoptosis (Tolkovsky et al., 2002).

## Speculation about the mechanism of stopping events

Stopping events cluster between docked mitochondria. For this to occur, it seems likely there is a gradient in a molecule that docked mitochondria create. This could be an ion such as $Ca^{2+}$ (Budd and Nicholls, 1996; Kanai et al., 2001; Kanje et al., 1981; Kendal et al., 1983; Ochs and Jersild, 1984; Ochs et al., 1977), a metabolite such as ATP (de Graaf et al., 2000), creatine (van Deursen et al., 1993), ADP or NADH (Bereiter-Hahn and Voth, 1983; Bereiter-Hahn and Voth, 1994), a second messenger such as a small G-protein (Alto et al., 2002; Fransson et al., 2003), or another signal-transduction pathway (Chada and Hollenbeck, 2003). It follows that the concentration of the molecule alters a sensor that regulates activity of a motor (as discussed below) or linker between the mitochondria and cytoskeleton (Boldogh et al., 1998; Trinczek et al., 1999; Wagner et al., 2003). The sensor could be either positioned in the cytoplasm or associated with the mitochondria. The results of the mannitol experiment suggest that mitochondrial stopping might be related to axonal ionic conditions. The observations that docked mitochondria have a mixed potential and that mitochondrial potential is not tightly correlated with stopping events (Fig. 7) suggest that docking and the direction of transport are independently regulated.

## Speculation about the mechanism of transport regulation

The mechanisms of directional transport regulation must include a sensor. Possibilities include a mitochondrial membrane sensor of mitochondrial potential, the flux or concentration of a metabolite or ion such as $H^+$, $Ca^{2+}$, ATP, ADP, pyruvate or NADH, or the conformation of proteins that indirectly sense mitochondrial potential. The sensor could be associated with the mitochondria or be cytoplasmic. A review by Nicholls and Budd (Nicholls and Budd, 2000) presents a good picture of the complexity of mitochondrial function and the diverse effects associated with alterations in mitochondrial function. After modulation of the sensor, a signal must be sent in a manner that coordinates the regulation of the anterograde and retrograde motors.

Mitochondria are transported in the anterograde direction by kinesins (Nangaku et al., 1994; Pereira et al., 1997; Tanaka et al., 1998), and levels of kinesin-mediated transport are correlated with the phosphorylation state of both heavy and light chains (De Vos et al., 1998; De Vos et al., 2000; Lee and Hollenbeck, 1995; Lindesmith et al., 1997; Matthies et al., 1993; McIlvain et al., 1994; Sato-Yoshitake et al., 1992). There are separate signal-transduction pathways responsible for the transport of mitochondria and other organelles (Okada et al., 1995). A particularly interesting pathway involves tumor necrosis factor (TNF) (Baud and Karin, 2001). Treatment with TNF leads to apoptosis and perinuclear clustering of the mitochondria (De Vos et al., 1998; Luo et al., 1998). The perinuclear clustering of the mitochondria is correlated with hyperphosphorylation of kinesin light chain and inhibition of kinesin-mediated mitochondrial motility (De Vos et al., 2000). This work raises the question of whether the depolarization of the mitochondria through TNF's effect on caspase-8 and apoptosis leads to hyperphosphorylation of the kinesin or whether levels of kinesin activity are regulated by a separate pathway (Baud and Karin, 2001).

Dynein might be the retrograde motor that transports mitochondria (Habermann et al., 2001), but mitochondrial transport is not regulated through dynactin (Burkhardt et al., 1997). This raises the question of how mitochondrial potential relates to dynein-dependent transport. Tctex1 is a dynein light chain that is capable of supporting dynein-mediated transport (Tai et al., 1999). In a yeast two-hybrid screen, it has been shown to interact with the voltage-dependent anion-selective channel (VDAC) (Schwarzer et al., 2002). VDAC is the major channel for the movement of adenine nucleotides for the mitochondria. Presuming a link between anion flux through VDAC, VDAC conformation and mitochondrial potential, the VDAC-Tctex1 interaction is an appealing yet preliminary candidate for the regulation of dynein mediated mitochondrial transport.

How microtubule motors are coordinately regulated is an important long-term question (Gross et al., 2002; Huang et al., 1999). Previously, we demonstrated that the direction but not the level of mitochondrial transport is modulated through a pathway that involves phosphatidylinositol (De Vos et al., 2003). The results presented here suggest that the direction of mitochondrial transport in the axon is regulated to ensure that mitochondria with high potential are transported out into the axon, and old or damaged mitochondria with low potential are transported back to the cell body.

## Conclusions

In this paper, we have shown that a uniform distribution of mitochondria is generated by the regulation of mitochondrial stopping events, that the direction of mitochondrial transport is correlated with mitochondrial potential and that an inhibitor of complex III of the electron transport chain, antimycin, induces retrograde mitochondrial transport.

## References

**Allen, R. D., Metuzals, J., Tasaki, I., Brady, S. T. and Gilbert, S. P.** (1982). Fast axonal transport in squid giant axon. *Science* **218**, 1127-1129.

**Alto, N. M., Soderling, J. and Scott, J. D.** (2002). Rab32 is an A-kinase anchoring protein and participates in mitochondrial dynamics. *J. Cell Biol.* **158**, 659-668.

**Banker, G. and Goslin, K.** (1998). *Culturing nerve cells*. Cambridge, MA: MIT Press.

**Baud, V. and Karin, M.** (2001). Signal transduction by tumor necrosis factor and its relatives. *Trends Cell Biol.* **11**, 372-377.

**Bereiter-Hahn, J. and Voth, M.** (1983). Metabolic control of shape and structure of mitochondria in situ. *Biol. Cell* **47**, 309-322.

**Bereiter-Hahn, J. and Voth, M.** (1994). Dynamics of mitochondria in living cells, shape changes, dislocations, fusion, and fission of mitochondria. *Microsc. Res. Tech.* **27**, 198-219.

**Bindokas, V. P., Lee, C. C., Colmers, W. F. and Miller, R. J.** (1998). Changes in mitochondrial function resulting from synaptic activity in the rat hippocampal slice. *J. Neurosci.* **18**, 4570-4587.

**Boldogh, I., Vojtov, N., Karmon, S. and Pon, L. A.** (1998). Interaction between mitochondria and the actin cytoskeleton in budding yeast requires two integral mitochondrial outer membrane proteins, Mmm1p and Mdm10p. *J. Cell Biol.* **141**, 1371-1381.

**Borgdorff, A. J., Somjen, G. G. and Wadman, W. J.** (2000). Two mechanisms that raise free intracellular calcium in rat hippocampal neurons during hypoosmotic and low NaCl treatment. *J. Neurophysiol.* **83**, 81-89.

**Budd, S. L. and Nicholls, D. G.** (1996). A reevaluation of the role of mitochondria in neuronal $Ca^{2+}$ homeostasis. *J. Neurochem.* **66**, 403-411.

**Burkhardt, J. K., Echeverri, C. J., Nilsson, T. and Vallee, R. B.** (1997). Overexpression of the dynamitin (p50) subunit of the dynactin complex disrupts dynein-dependent maintenance of membrane organelle distribution. *J. Cell Biol.* **139**, 469-484.

**Burton, P. R. and Paige, J. L.** (1981). Polarity of axoplasmic microtubules in the olfactory nerve of the frog. *Proc. Natl. Acad. Sci. USA* **78**, 3269-3273.

**Chada, S. R. and Hollenbeck, P. J.** (2003). Mitochondrial movement and positioning in axons, the role of growth factor signaling. *J. Exp. Biol.* **206**, 1985-1992.

**Collins, T. J., Berridge, M. J., Lipp, P. and Bootman, M. D.** (2002). Mitochondria are morphologically and functionally heterogeneous within cells. *EMBO J.* **21**, 1616-1627.

**Cunarro, J. and Weiner, M. W.** (1975). Mechanism of action of agents which uncouple oxidative phosphorylation, direct correlation between proton-carrying and respiratory-releasing properties using rat liver mitochondria. *Biochim. Biophys. Acta Mol. Cell Res.* **387**, 234-240.

**Davis, A. F. and Clayton, D. A.** (1996). In situ localization of mitochondrial DNA replication in intact mammalian cells. *J. Cell Biol.* **135**, 883-893.

**de Graaf, R. A., van Kranenburg, A. and Nicolay, K.** (2000). In vivo (31)P-NMR diffusion spectroscopy of ATP and phosphocreatine in rat skeletal muscle. *Biophys. J.* **78**, 1657-1664.

**De Vos, K., Goossens, V., Boone, E., Vercammen, D., Vancompernolle, K., Vandenabeele, P., Haegeman, G., Fiers, W. and Grooten, J.** (1998). The 55-kDa tumor necrosis factor receptor induces clustering of mitochondria through its membrane-proximal region. *J. Biol. Chem.* **273**, 9673-9680.

**De Vos, K., Severin, F., van Herreweghe, F., Vancompernolle, K., Goossens, V., Hyman, A. and Grooten, J.** (2000). Tumor necrosis factor induces hyperphosphorylation of kinesin light chain and inhibits kinesin-mediated transport of mitochondria. *J. Cell Biol.* **149**, 1207-1214.

**De Vos, K. J., Sable, J., Miller, K. E. and Sheetz, M. P.** (2003). Expression of phosphatidylinositol (4,5) bisphosphate-specific pleckstrin homology domains alters direction but not the level of axonal transport of mitochondria. *Mol. Biol. Cell* **14**, 3636-3649.

**Desagher, S. and Martinou, J. C.** (2000). Mitochondria as the central control point of apoptosis. *Trends Cell Biol.* **10**, 369-377.

**Ferhat, L., Kuriyama, R., Lyons, G. E., Micales, B. and Baas, P. W.** (1998). Expression of the mitotic motor protein CHO1/MKLP1 in postmitotic neurons. *Eur. J. Neurosci.* **10**, 1383-1393.

**Feynman, R. P., Leighton, R. B. and Sands, M. L.** (1963). *The Feynman Lectures on Physics*. Reading, MA: Addison-Wesley.

**Fishman, R. A., Reiner, M. and Chan, P. H.** (1977). Metabolic changes associated with iso-osmotic regulation in brain cortex slices. *J. Neurochem.* **28**, 1061-1067.

**Fransson, A., Ruusala, A. and Aspenstrom, P.** (2003). Atypical Rho GTPases have roles in mitochondrial homeostasis and apoptosis. *J. Biol. Chem.* **278**, 6495-6502.

**Friede, R. L. and Ho, K. C.** (1977). The relation of axonal transport of mitochondria with microtubules and other axoplasmic organelles. *J. Physiol.* **265**, 507-519.

**Gross, S. P., Welte, M. A., Block, S. M. and Wieschaus, E. F.** (2002). Coordination of opposite-polarity microtubule motors. *J. Cell Biol.* **156**, 715-724.

**Gunawardena, S. and Goldstein, L. S.** (2001). Disruption of axonal transport and neuronal viability by amyloid precursor protein mutations in *Drosophila*. *Neuron* **32**, 389-401.

**Gunawardena, S., Her, L. S., Brusch, R. G., Laymon, R. A., Niesman, I. R., Gordesky-Gold, B., Sintasath, L., Bonini, N. M. and Goldstein, L. S.** (2003). Disruption of axonal transport by loss of huntingtin or expression of pathogenic polyQ proteins in *Drosophila*. *Neuron* **40**, 25-40.

**Ha, H.** (1970). Axonal bifurcation in the dorsal root ganglion of the cat, a light and electron microscopic study. *J. Comp. Neurol.* **140**, 227-240.

**Habermann, A., Schroer, T. A., Griffiths, G. and Burkhardt, J. K.** (2001). Immunolocalization of cytoplasmic dynein and dynactin subunits in cultured macrophages, enrichment on early endocytic organelles. *J. Cell Sci.* **114**, 229-240.

**Hagen, T. M., Yowe, D. L., Bartholomew, J. C., Wehr, C. M., Do, K. L., Park, J. Y. and Ames, B. N.** (1997). Mitochondrial decay in hepatocytes from old rats, membrane potential declines, heterogeneity and oxidants increase. *Proc. Natl. Acad. Sci. USA* **94**, 3064-3069.

**Heidemann, S. R., Landers, J. M. and Hamborg, M. A.** (1981). Polarity orientation of axonal microtubules. *J. Cell Biol.* **91**, 661-665.

**Hollenbeck, P. J.** (1993). Products of endocytosis and autophagy are retrieved from axons by regulated retrograde organelle transport. *J. Cell Biol.* **121**, 305-315.

**Hollenbeck, P. J.** (1996). The pattern and mechanism of mitochondrial transport in axons. *Front. Biosci.* **1**, 91-102.

**Hollenbeck, P. J. and Bray, D.** (1987). Rapidly transported organelles containing membrane and cytoskeletal components, their relation to axonal growth. *J. Cell Biol.* **105**, 2827-2835.

**Hollenbeck, P. J., Bray, D. and Adams, R. J.** (1985). Effects of the uncoupling agents FCCP and CCCP on the saltatory movements of cytoplasmic organelles. *Cell Biol. Int. Rep.* **9**, 193-199.

**Huang, J. D., Brady, S. T., Richards, B. W., Stenolen, D., Resau, J. H., Copeland, N. G. and Jenkins, N. A.** (1999). Direct interaction of microtubule- and actin-based transport motors. *Nature* **397**, 267-270.

**Hurd, D. D. and Saxton, W. M.** (1996). Kinesin mutations cause motor neuron disease phenotypes by disrupting fast axonal transport in *Drosophila*. *Genetics* **144**, 1075-1085.

**Huser, J. and Blatter, L. A.** (1999). Fluctuations in mitochondrial membrane potential caused by repetitive gating of the permeability transition pore. *Biochem. J.* **343**, 311-317.

**Kanai, A., Hiruma, H., Katakura, T., Sase, S., Kawakami, T. and Hoka, S.** (2001). Low-concentration lidocaine rapidly inhibits axonal transport in cultured mouse dorsal root ganglion neurons. *Anesthesiology* **95**, 675-680.

**Kaniuga, Z., Gardas, A. and Bryla, J.** (1968). Studies on the mechanism of inhibition of the mitochondrial electron transport by antimycin. I. Reversal of the inhibition by diethyl ether extraction. *Biochim. Biophys. Acta Mol. Cell Res.* **153**, 60-69.

**Kanje, M., Edstrom, A. and Hanson, M.** (1981). Inhibition of rapid axonal transport in vitro by the ionophores X-537 A and A 23187. *Brain Res.* **204**, 43-50.

**Kendal, W. S., Koles, Z. J. and Smith, R. S.** (1983). Oscillatory motion of intra-axonal organelles of *Xenopus laevis* following inhibition of their rapid transport. *J. Physiol.* **345**, 501-513.

**Klionsky, D. J. and Emr, S. D.** (2000). Autophagy as a regulated pathway of cellular degradation. *Science* **290**, 1717-1721.

**Lee, K. D. and Hollenbeck, P. J.** (1995). Phosphorylation of kinesin in vivo correlates with organelle association and neurite outgrowth. *J. Biol. Chem.* **270**, 5600-5605.

**Lemasters, J. J., Nieminen, A. L., Qian, T., Trost, L. C., Elmore, S. P., Nishimura, Y., Crowe, R. A., Cascio, W. E., Bradham, C. A., Brenner, D. A. et al.** (1998). The mitochondrial permeability transition in cell death, a common mechanism in necrosis, apoptosis and autophagy. *Biochim. Biophys. Acta Mol. Cell Res.* **1366**, 177-196.

**Ligon, L. A. and Steward, O.** (2000). Movement of mitochondria in the axons and dendrites of cultured hippocampal neurons. *J. Comp. Neurol.* **427**, 340-350.

**Lindesmith, L., McIlvain, J. M., Jr, Argon, Y. and Sheetz, M. P.** (1997). Phosphotransferases associated with the regulation of kinesin motor activity. *J. Biol. Chem.* **272**, 22929-22933.

**Luo, X., Budihardjo, I., Zou, H., Slaughter, C. and Wang, X.** (1998). Bid, a Bcl2 interacting protein, mediates cytochrome c release from mitochondria in response to activation of cell surface death receptors. *Cell* **94**, 481-490.

**Martenson, C. H., Odom, A., Sheetz, M. P. and Graham, D. G.** (1995). The effect of acrylamide and other sulfhydryl alkylators on the ability of dynein and kinesin to translocate microtubules in vitro. *Toxicol. Appl. Pharmacol.* **133**, 73-81.

**Matthies, H. J., Miller, R. J. and Palfrey, H. C.** (1993). Calmodulin binding to and cAMP-dependent phosphorylation of kinesin light chains modulate kinesin ATPase activity. *J. Biol. Chem.* **268**, 11176-11187.

**McIlvain, J. M., Jr, Burkhardt, J. K., Hamm-Alvarez, S., Argon, Y. and**

**Sheetz, M. P.** (1994). Regulation of kinesin activity by phosphorylation of kinesin-associated proteins. *J. Biol. Chem.* **269**, 19176-19182.

**Menzies, R. A. and Gold, P. H.** (1971). The turnover of mitochondria in a variety of tissues of young adult and aged rats. *J. Biol. Chem.* **246**, 2425-2429.

**Minamikawa, T., Sriratana, A., Williams, D. A., Bowser, D. N., Hill, J. S. and Nagley, P.** (1999). Chloromethyl-X-rosamine (MitoTracker Red) photosensitises mitochondria and induces apoptosis in intact human cells. *J. Cell Sci.* **112**, 2419-2430.

**Morris, R. L. and Hollenbeck, P. J.** (1993). The regulation of bidirectional mitochondrial transport is coordinated with axonal outgrowth. *J. Cell Sci.* **104**, 917-927.

**Nangaku, M., Sato-Yoshitake, R., Okada, Y., Noda, Y., Takemura, R., Yamazaki, H. and Hirokawa, N.** (1994). KIF1B, a novel microtubule plus end-directed monomeric motor protein for transport of mitochondria. *Cell* **79**, 1209-1220.

**Nicholls, D. G. and Budd, S. L.** (2000). Mitochondria and neuronal survival. *Physiol. Rev.* **80**, 315-360.

**Ochs, S. and Hollingsworth, D.** (1971). Dependence of fast axoplasmic transport in nerve on oxidative metabolism. *J. Neurochem.* **18**, 107-114.

**Ochs, S. and Jersild, R. A., Jr** (1984). Calcium localization in nerve fibers in relation to axoplasmic transport. *Neurochem. Res.* **9**, 823-836.

**Ochs, S. and Smith, C. B.** (1971). Fast axoplasmic transport in mammalian nerve in vitro after block of glycolysis with iodoacetic acid. *J. Neurochem.* **18**, 833-843.

**Ochs, S., Worth, R. M. and Chan, S. Y.** (1977). Calcium requirement for axoplasmic transport in mammalian nerve. *Nature* **270**, 748-750.

**Okada, Y., Sato-Yoshitake, R. and Hirokawa, N.** (1995). The activation of protein kinase A pathway selectively inhibits anterograde axonal transport of vesicles but not mitochondria transport or retrograde transport in vivo. *J. Neurosci.* **15**, 3053-3064.

**Overly, C. C., Rieff, H. I. and Hollenbeck, P. J.** (1996). Organelle motility and metabolism in axons vs dendrites of cultured hippocampal neurons. *J. Cell Sci.* **109**, 971-980.

**Papa, S.** (1996). Mitochondrial oxidative phosphorylation changes in the life span. Molecular aspects and physiopathological implications. *Biochim. Biophys. Acta Mol. Cell Res.* **1276**, 87-105.

**Pereira, A. J., Dalby, B., Stewart, R. J., Doxsey, S. J. and Goldstein, L. S.** (1997). Mitochondrial association of a plus end-directed microtubule motor expressed during mitosis in *Drosophila*. *J. Cell Biol.* **136**, 1081-1090.

**Pilatus, U., Aboagye, E., Artemov, D., Mori, N., Ackerstaff, E. and Bhujwalla, Z. M.** (2001). Real-time measurements of cellular oxygen consumption, pH, and energy metabolism using nuclear magnetic resonance spectroscopy. *Magn. Reson. Med.* **45**, 749-755.

**Reers, M., Smith, T. W. and Chen, L. B.** (1991). J-aggregate formation of a carbocyanine as a quantitative fluorescent indicator of membrane potential. *Biochemistry* **30**, 4480-4486.

**Rizzuto, R.** (2001). Intracellular Ca(2+) pools in neuronal signalling. *Curr. Opin. Neurobiol.* **11**, 306-311.

**Rottenberg, H. and Wu, S.** (1998). Quantitative assay by flow cytometry of the mitochondrial membrane potential in intact cells. *Biochim. Biophys. Acta Mol. Cell Res.* **1404**, 393-404.

**Sato-Yoshitake, R., Yorifuji, H., Inagaki, M. and Hirokawa, N.** (1992). The phosphorylation of kinesin regulates its binding to synaptic vesicles. *J. Biol. Chem.* **267**, 23930-23936.

**Schwarzer, C., Barnikol-Watanabe, S., Thinnes, F. P. and Hilschmann, N.** (2002). Voltage-dependent anion-selective channel (VDAC) interacts with the dynein light chain Tctex1 and the heat-shock protein PBP74. *Int. J. Biochem. Cell Biol.* **34**, 1059-1070.

**Smiley, S. T., Reers, M., Mottola-Hartshorn, C., Lin, M., Chen, A., Smith, T. W., Steele, G. D., Jr and Chen, L. B.** (1991). Intracellular heterogeneity in mitochondrial membrane potentials revealed by a J-aggregate-forming lipophilic cation JC-1. *Proc. Natl. Acad. Sci. USA* **88**, 3671-3675.

**Stowers, R. S., Megeath, L. J., Gorska-Andrzejak, J., Meinertzhagen, I. A. and Schwarz, T. L.** (2002). Axonal transport of mitochondria to synapses depends on Milton, a novel *Drosophila* protein. *Neuron* **36**, 1063-1077.

**Tai, A. W., Chuang, J. Z., Bode, C., Wolfrum, U. and Sung, C. H.** (1999). Rhodopsin's carboxy-terminal cytoplasmic tail acts as a membrane receptor for cytoplasmic dynein by binding to the dynein light chain Tctex-1. *Cell* **97**, 877-887.

**Tanaka, Y., Kanai, Y., Okada, Y., Nonaka, S., Takeda, S., Harada, A. and Hirokawa, N.** (1998). Targeted disruption of mouse conventional kinesin heavy chain, Kif5B, results in abnormal perinuclear clustering of mitochondria. *Cell* **93**, 1147-1158.

**Terasaki, M. and Reese, T. S.** (1992). Characterization of endoplasmic reticulum by co-localization of BiP and dicarbocyanine dyes. *J. Cell Sci.* **101**, 315-322.

**Tolkovsky, A. M., Xue, L., Fletcher, G. C. and Borutaite, V.** (2002). Mitochondrial disappearance from cells, a clue to the role of autophagy in programmed cell death and disease? *Biochimie* **84**, 233-240.

**Trinczek, B., Ebneth, A., Mandelkow, E. M. and Mandelkow, E.** (1999). Tau regulates the attachment/detachment but not the speed of motors in microtubule-dependent transport of single vesicles and organelles. *J. Cell Sci.* **112**, 2355-2367.

**Tzung, S. P., Kim, K. M., Basanez, G., Giedt, C. D., Simon, J., Zimmerberg, J., Zhang, K. Y. and Hockenbery, D. M.** (2001). Antimycin A mimics a cell-death-inducing Bcl-2 homology domain 3. *Nat. Cell Biol.* **3**, 183-191.

**van Deursen, J., Heerschap, A., Oerlemans, F., Ruitenbeek, W., Jap, P., ter Laak, H. and Wieringa, B.** (1993). Skeletal muscles of mice deficient in muscle creatine kinase lack burst activity. *Cell* **74**, 621-631.

**Wagner, O. I., Lifshitz, J., Janmey, P. A., Linden, M., McIntosh, T. K. and Leterrier, J. F.** (2003). Mechanisms of mitochondria-neurofilament interactions. *J. Neurosci.* **23**, 9046-9058.

**Wong-Riley, M. T.** (1989). Cytochrome oxidase, an endogenous metabolic marker for neuronal activity. *Trends Neurosci.* **12**, 94-101.

**Xue, L., Fletcher, G. C. and Tolkovsky, A. M.** (2001). Mitochondria are selectively eliminated from eukaryotic cells after blockade of caspases during apoptosis. *Curr. Biol.* **11**, 361-365.

**Zar, J. H.** (1999). *Biostatistical Analysis*. Upper Saddler River, NJ: Prentice Hall.

**Zhou, H. M., Brust-Mascher, I. and Scholey, J. M.** (2001). Direct visualization of the movement of the monomeric axonal transport motor UNC-104 along neuronal processes in living *Caenorhabditis elegans*. *J. Neurosci.* **21**, 3749-3755.